Boson peak in the Raman spectra of amorphous gallium arsenide: Generalization to amorphous tetrahedral semiconductors

M. Ivanda,* I. Hartmann, and W. Kiefer
Institut für Physikalische Chemie, Universität Würzburg, Marcusstraße 9-11, D-97070 Würzburg, Federal Republic of Germany
(Received 13 January 1994; revised manuscript received 5 July 1994)

We report on the observation of the boson peak in amorphous (*a*) GaAs formed by high-energy ion bombardment of the crystalline lattice. The experimental data are analyzed according to the theory of inelastic light scattering from fractons. The correlation length ξ and the spectral dimension $\tilde{d}$ of the fractal are determined. In comparison to *a*-Si:H the crossover frequency from the phonon to the fracton scattering regime, ω_{co1}, is lower and scales according to mass law, confirming the vibrational character of the boson peak. The origin of the fractals in tetrahedral amorphous semiconductors is discussed in terms of strained nanometer blobs of host atoms whose overcoordination is relaxed through bond percolation. The intensity increase of the boson peak relative to the amorphous component during the process of amorphization of GaAs, and the increase in the carbon content in *a*-Si:H, shows a composite structure that consists of a strained fractal region in the relaxed network. Some experimentally observed anomalies such as low values of the sound velocity in tetrahedral amorphous semiconductors, and transformation of the vibrational spectrum by quenching in As_2S_3 are qualitatively explained by the fractal model. On the basis of maximum positions of the boson peak and the first sharp diffraction peak observed in the structure factor of inelastic x-ray or neutron scattering of amorphous semiconductors, the correlation lengths of medium-range order (MRO) are determined and compared for different tetrahedral and vitreous amorphous semiconductors. The observed three to four times shorter value of MRO in tetrahedral relative to vitreous amorphous semiconductors is used to explain a number of differences between their properties.

I. INTRODUCTION

A great number of experimental results show that many properties of liquids and amorphous solids (excitation and relaxation kinetics, thermal, optical, and electron processes) depend on structural features at length scale from atomic level to a few hundred Å.[1–12] This so-called local or medium-rangle order (MRO) depends on the material and conditions of formation. The range of MRO, its relation to physical properties, and its dependence on the kinetics of formation of the solid are questions of interest in basic solid-state physics, in fabricating materials for harnessing solar energy, in polymer science, and in relating the structure of biological molecules to their function.

The first-order Raman spectrum of disorder form of a material contains in principle more information than the first-order Raman spectrum of the corresponding crystal. The absence of translation symmetry or long-range order relaxes the selection rules so that all phonons in the Brillouin zone participate in the first-order Raman scattering.[13] Therefore, the low-frequency Raman-scattering spectroscopy may be an efficient method for the investigation of structural properties at all length scales of noncrystalline solids. Especially, there is great interest in the analysis of Raman spectra where the MRO is manifested through the boson peak.

Recently, it has been estimated that the structural features of MRO cause the excess of the phonon density of states (PDOS) in comparison to the expected Debye value which is responsible for the observation of the so-called boson peak.[14–17] The theory of inelastic scattering from fractons shows that the excess of the PDOS can be understood on the basis of strongly localized vibrational excitation of the self-similar fractal structure.[18–20] While the theory of fractal vibrations has been strongly confirmed by a series of experiments on low-density materials such as silica aerogels,[21] the existence of fractals in denser systems such as polymers, glasses, and amorphous solids has not been established. For stronger evidence more experimental work is needed. In particular, it is interesting to know both the density of vibrational states and the shape and extension of the localized vibrational wave functions which determine thermal and transport properties.

Due to their wide application, the research on amorphous semiconductors has attracted considerable attention. According to their properties they are divided into the two classes: vitreouslike *a*-Se or *a*-As_2S_3, and tetrahedral-like *a*-Si or *a*-GaAs.[22] It is believed that the origin of their differences lie in MRO, but is still not clear enough. While the boson peak was observed in the vitreous amorphous semiconductor in its common spectral form, in tetrahedral semiconductors it was only identified with a transversal acoustical (TA) phonon vibrational band.[23] On the other hand, the origin of the TA band is well explained by disorder-induced broadening of the crystalline phonon density of states, and by the numerical calculation of PDOS based on the model of periodic continuous random network (CRN).[24] Therefore, the TA

phonon vibrational band could not be ascribed to the boson peak whose origin is in some unknown structural features at the length scale of MRO. Recently, one of us has found the boson peak in amorphous hydrogenated silicon (*a*-Si:H) with the same spectral form as observed in glassy solids.[25] To show evidence that the boson peak generally exists in tetrahedral amorphous semiconductors in its common form, we show here that it also exists in tetrahedral *a*-GaAs. The boson peak is analyzed in the frame of the fractal model. In Sec. II experimental conditions for the sample preparation and Raman measurements are presented. In Sec. III the bosonlike character of the broad background signal (BBS) and its similarity to the boson peak observed in glassy solids are shown. In Sec. IV the theory of Raman scattering from fractal vibrations is applied for the explanation of the BBS. The origin of fractals is discussed in terms of strained nanometer-sized blobs of host atoms, and some peculiarities observed in amorphous semiconductors are qualitatively explained by the fractal model. In Sec. V a structural correlation determined from the boson peak and the first sharp diffraction peak (FSDP) observed in the structural factor of inelastic x-ray or neutron scattering are compared for different amorphous semiconductors. A conclusion about the MRO and its reflection on structural properties of amorphous semiconductors is drawn. A summary and conclusions are given in Sec. VI.

II. EXPERIMENT

Commercial undoped GaAs (100) wafers were implanted with 100-keV Si^+ ions. During implantation the substrate was tilted 7° with respect to the incident beam to minimize the channeling effects. The applied ion dose was in the range from 1×10^{14} to 3×10^{15} cm^{-2}. According to ion channeling measurements,[26] the highest applied ion dose ensures the layer to be completely amorphized.

Amorphous hydrogenated silicon thin films with variable carbon content were prepared by means of dc magnetron sputtering on a silicon (111) substrate of 200 μm thickness at room temperature. Sputtering was performed in gaseous mixture of Ar, H_2, and benzene vapor with partial pressures of 1.33, 0.5, and 0–0.381 Pa, respectively. Deposition rate was $\sim$100 Å/min, and film thickness was $\sim$1.3 μm.

The Raman spectra of samples evacuated to 10^{-4} Torr were recorded by means of a DILOR Z-24 triple spectrometer in a right-angle-scattering geometry. The spectrometer slits were set to 800 μm which corresponds to a spectral width of $\approx$7 cm^{-1}. The excitation light, $\lambda=5145$ Å, was emitted from a COHERENT INNOVA 100 Ar-ion laser. The laser power of 0.5 W for GaAs and 1.5 W for *a*-$Si_{1-x}C_x$:H samples was focused to form an eliptical spot with dimensions 100×400 μm^2. The HH and HV polarized Raman spectra were taken in a single scan, and with a signal accumulation time of 3 s. The HH(V) polarization means horizontally polarized incident light and horizontally (vertically) analyzed scattered light with respect to the scattering plane. The spectrum of the background was recorded separately and removed from the Raman spectra of the samples. The spectra were then radiometrically (for the spectrometer throughput) corrected and temperature reduced by the boson occupation number as follows: $I_R=I/[n(\omega,T)+1]$, where $n(\omega,T)$ is the Bose-Einstein factor.

For the low-temperature measurements, the sample was cooled with a helium closed-cycle CTi CRYODNE cryostat down to 10 K. In order to avoid undue heating of the sample the laser power was reduced to 200 mW, but accumulation time of the Raman signal was increased to 60 s. The mean temperature of the exposed part of the sample was determined from the Stokes/anti-Stokes ratio of the Raman scattering intensity of TO phonon vibrational band at 260 cm^{-1}.

III. BOSON CHARACTER OF THE BROAD BACKGROUND SIGNAL

In this section, by the similar methods as presented in a recent paper,[25] we show that properties of the BBS are the same as of the boson peak observed in glassy and vitreous amorphous semiconductors. Figure 1 shows Raman spectra of *a*-GaAs recorded at HH and HV polarization geometry. Figure 1(a) shows uncorrected, Fig. 1(b) corrected for the spectrometer response, and Fig. 1(c) corrected for the spectrometer response and temperature-reduced Raman spectra. It is evident that the vibrational bands are superimposed on the BBS. In the case of the bosonlike character of the excitation, the Stokes/anti-Stokes ratio of the Raman scattering intensi-

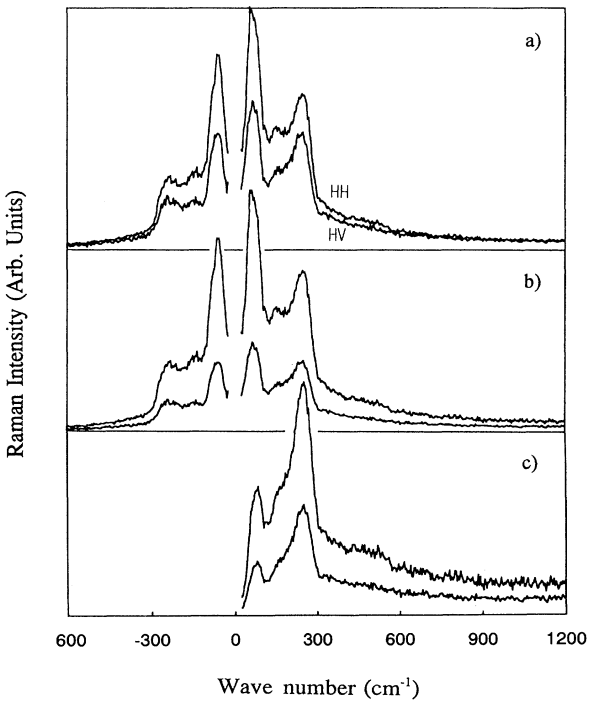

FIG. 1. Polarized Raman spectra of *a*-GaAs radiometrically (a) uncorrected, (b) corrected, (c) corrected and temperature reduced.

ty must obey the following relation:

$$I_S/I_{As}(\omega,t)=\left[\frac{\omega_L-\omega}{\omega_L+\omega}\right]^3 \exp\left[\frac{\hbar\omega}{kT}\right], \quad (1)$$

where ω_L is the laser excitation angular frequency, ω the phonon angular frequency, and T the absolute temperature. Figure 2 shows that Eq. (1) is satisfied for all vibrations in the frequency range up to 700 cm^{-1}, and as shown in Fig. 3 in the temperature range from 50 to 370 K for phonon wave numbers at 70 and 260 cm^{-1}, and wave number of the BBS at 125 cm^{-1}.

The depolarization ratio spectrum $\rho(\omega)$ of the BBS shown in Fig. 4 as a function of wave number is nearly constant (≈ 0.43) in the whole spectral range analyzed. The observed local minima at ≈ 70 cm^{-1} and at ≈ 260 cm^{-1} are influenced by the depolarization ratio of TA and TO phonon vibrational bands. Similar properties of the depolarization ratio, and also of the asymmetric spectral shape of the BBS as shown in Fig. 5, have been observed on boson peak in liquids[27] and glassy solids.[8] This allows us to consider the BBS as a boson peak.

A number of models have been proposed for the explanation of the boson peak: coupled rotation of SiO_4 tetrahedra in v-SiO_2,[14] involvement of local vibrational modes of nanocrystalline clusters,[16] dipolar interactions between some defects,[28] involvement of soft anharmonic potentials,[29] and fractonlike dynamics of fractal structure.[30]

There are several reasons for the acceptance of fractal model for the explanation of the boson peak in amorphous semiconductors: (a) formation of the fractal structure during the layer deposition or by high-energy ion bombardment seems plausible and it is confirmed by recent scanning tunneling microscopy and atomic-force microscopy experiments[31,32]; (b) some experimentally observed phenomena in a-Si:H which are fundamentally difficult to explain by traditional models have been qualitatively well explained in terms of fractal geometry;[33] (c) thermal properties, plato in thermal conductivity, excess of heat capacity, and boson peak in some of amorphous and glassy solids have been quantitatively explained by fractal model;[20,34–38] (d) constant value of the depolarization ratio of the boson peak which is hard to explain by the homogeneous Euclidian structure in such a large spectral interval; in fractal structure due to self-similar anisotropy of the vibrating region it is expected to be equal at all localization length of the fractal vibrations;[39,40] (e) an anomalously long-phonon lifetime ob-

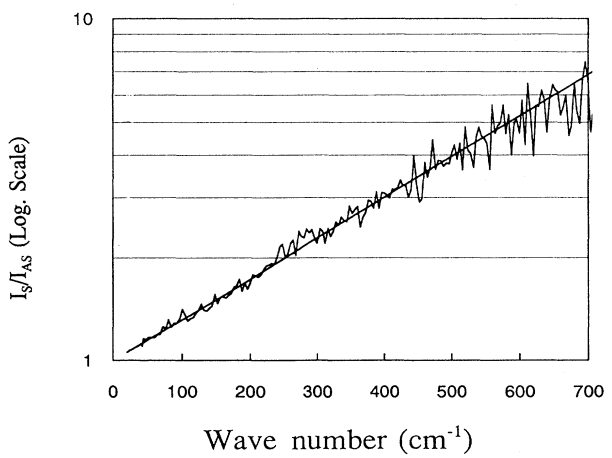

FIG. 2. Stokes/anti-Stokes ratio of the HV-polarized Raman intensity as a function of wave number. Straight line result from expected values for the boson character of the excitation.

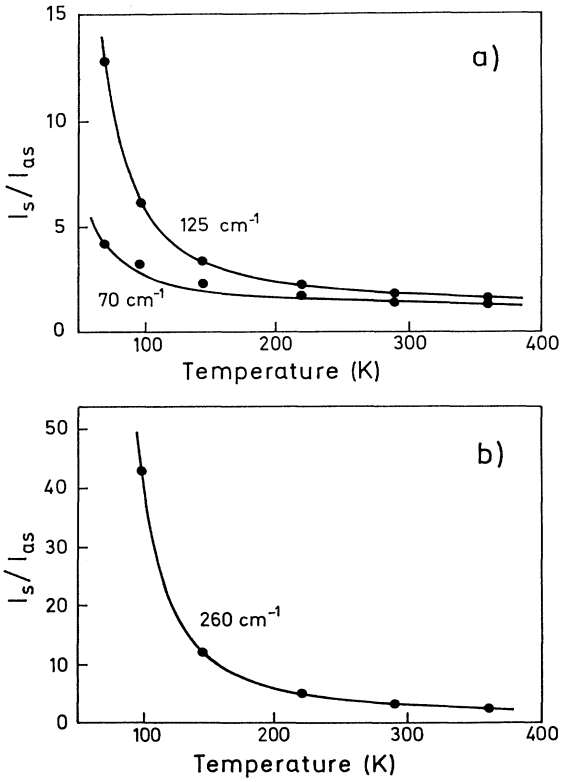

FIG. 3. Temperature dependence of the Stokes/anti-Stokes Ratio of the HV-polarized Raman intensity at different wavenumbers: (a) 70 and 125 cm^{-1} and (b) at 260 cm^{-1}. The lines are expected values according to boson character of excitation.

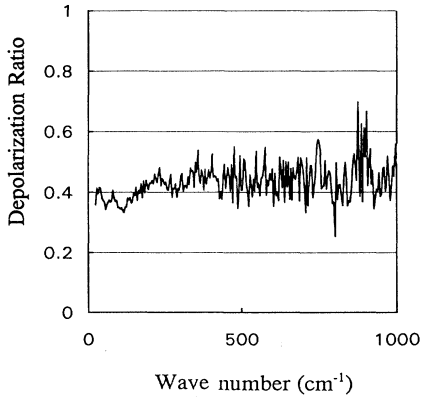

FIG. 4. Depolarization rate of a-GaAs as a function of wave number: $\rho(\omega)=I_{HV}/I_{HH}$.

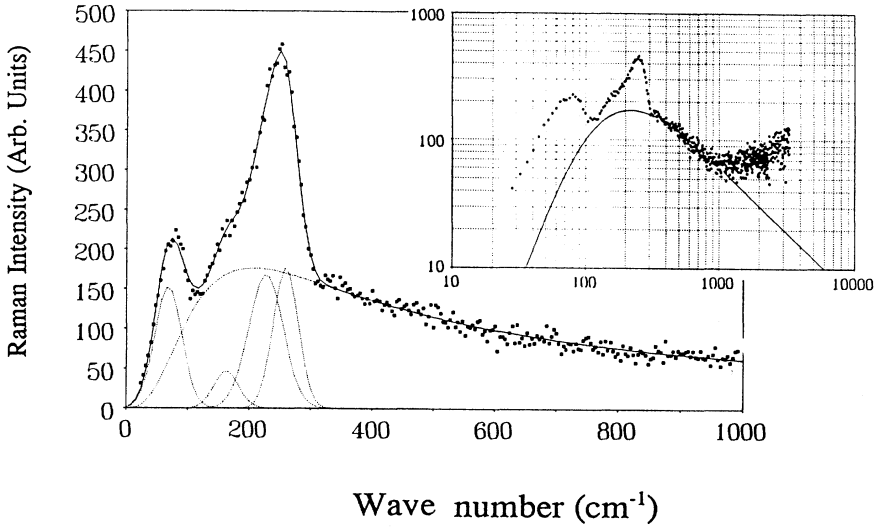

FIG. 5. Temperature-reduced HV-polarized Raman spectrum and fitted TA, II A, LO, and TO Gaussian-shaped phonon bands and phonon-fracton curve according to the fracton model. The inset shows the reduced Raman spectrum and fitted boson peak (solid line) up to 3000 cm^{-1} in log-log coordinates.

served in *a*-Si:H which is explained by strong phonons localization whose origin was proposed to be in fractal structure.[41]

IV. INTERPRETATION OF THE BOSON PEAK IN THE FRACTAL MODEL

The theory of Raman scattering from fractons is based on the dipole-induced dipole mechanism that has been recognized as the major source of Raman scattering in dense systems.[42,43] Considering the continuous transition from the phonon to the fracton scattering regime, the phonon-fracton curve of the temperature reduced Raman scattering intensity, $I^R(\omega)$, is given by[25]

$$I^R(\omega) \propto \omega^3(\omega^2+\omega_{co1}^2)^{[\tilde{d}/D(\sigma+d-D)-5/2]}, \quad (2)$$

where ω_{co1} is the crossover angular frequency from phonon to fracton scattering regime, $\tilde{d}$ the spectral dimension, D fractal dimension, d space dimension, and σ the scaling index describing the modulation of density in embedding space by the vibration.

Figure 5 shows the temperature reduced HV polarized Raman spectrum decomposed on the phonon-fracton curve and Gaussian shaped bands: TA at ≈ 70 cm^{-1}, II A at ≈ 160, LO at ≈ 230, and TO at ≈ 260 cm^{-1}. The results of fitting are presented in Table I together with the corresponding values found in *a*-Si:H.[25] While the fracton exponent is approximately the same, the crossover wave number together with the wave numbers of the phonon vibrational bands scale to lower values according to the mass law by a factor of ≈ 0.5, somewhat lower value than the expected value of 0.6 (maybe due to a small contribution of ionic type of bonding in GaAs). Scaling of ω_{co1} according to the mass law confirms the vibrational character of the BBS in tetrahedral amorphous semiconductors, and rules out the possibility of its origin as due to photoluminescence.

The correlation length ξ corresponding to the given crossover frequency is given by $\xi = v/(\omega_{co1}c)$, where c is the speed of light, and $v = 2.73 \times 10^5$ cm/s is the average sound velocity in *a*-GaAs. We used 58% of the mean value of the sound velocity in the crystalline state as observed for the sound velocities in *a*-Si and *a*-Ge.[44] The calculated value $\xi = 7.6$ Å, which is close to the correlation length in *a*-Si:H (≈ 6 Å), shows a small correlation length of fractals in *a*-GaAs. We note here that the value of ξ in ion-bombarded GaAs may also be related to the diameter of damaged region around the path of impinging ions. For Kr^+ and Be^+ ions, the estimated values are 10.2 and 4 Å, respectively.[45,46] Therefore, due to the fact that the size of damaged regions mainly depends on the diameter of impinging ion, one may expect some value in between for bombardment with Si^+ ions.

The fractal exponent is approximately equal to that found in *a*-Si:H. Using the same analysis as in Ref. 25, i.e., theoretical value $\sigma = 1.1$ for the scaling index,[42] and theoretical value for the fractal dimension of the percolating network $D = 2.5$,[47] we obtain $\tilde{d} = 0.77$ for the spectral dimension of fractal. It is comparable with the theoretical value $\tilde{d} = 0.9$ for the spectral dimension of tensorial elasticity calculated for the percolation clusters in three dimensions.[48]

The existence of fractals in amorphous and glassy solids sparked a debate that has not ended until now. For a percolating network the probability p for a bond or site occupation, the correlation length of fractal exhibits the scaling relation:[30] $\xi \simeq a|p-p_c|^{-\nu}$, where a is the smallest length scale in the fractal. In case of mass fractal and

TABLE I. Parameters from fitted phonon-fracton curves. The correlation lengths were calculated from the relation $\xi = v/(\omega_{co1}c)$, and the spectral dimension with the assumption $D = 2.5$.

	ω_{TO} (cm^{-1})	ω_{co1} (cm^{-1})	$(\sigma+d-D)\tilde{d}/D$	R (Å)	$\tilde{d}$
a-GaAs	260	120	0.49	7.6	0.77
c-Si:H	476	245	0.54	6	0.84
$\omega_{GaAs}/\omega_{Si}$	0.55	0.49			

percolation concentration above critical p_c, the correlation length ξ is determined by the size of the largest hole.[30] In a high-quality a-Si:H film the observed diameters of such holes are between 5 and 10 Å,[49] which correspond to the correlation length we found in a-Si:H.

On the other hand, the fact that the material does not exhibit a fractal static structure well may be irrelevant for fractal analysis.[20] It means that overall mass distribution may not be fractal (as it is not for a bond percolation network), but the bond network which contributes to the elasticity may be. That is, the dynamics are controlled by spectral dimension, while the total mass distribution may be equal or lower from Euclidean ($D < d$). Therefore, amorphous materials can be regarded as having a fractal force constant at short length scales. A fractal connectivity can be assumed for the masses which participate in the vibrational dynamics at length scales smaller than some characteristic length ξ.

According to the average coordination number of constitutive atoms $\langle r \rangle$, the amorphous solids can be either considered as overconstrained or underconstrained.[22] When $\langle r \rangle$ is between 2 and the characteristic value $r_p \approx 2.4$, the network is underconstrained and consists of rigid and floppy regions, but the rigid regions do not percolate. For $\langle r \rangle$ larger than r_p, the material is overconstrained and the rigid regions percolate. We suppose that the origin of fractals in amorphous and glassy solids are in such rigid regions. In the case of the self-similar fractal in connectivity, one should expect the elastic constant K to scale with length as $K \propto l^{-\alpha}$, where $\alpha = d - 2\sigma - D + 2D/\tilde{d}$.[39] With the values $\sigma = 1.1$, $D = 2.5$, and $\tilde{d} = 0.8$ (our value for the spectral dimension in tetrahedral amorphous semiconductors), one finds $\alpha = 4.5$. Using the above scaling relation we find that the elastic constants, defined as the coefficients of strain in the elastic deformation-energy density, are two orders of magnitude smaller on the surface of the fractal blobs than in the center, i.e., $K(7\text{ Å}) \approx 10^{-2} K(2.4\text{ Å})$. Therefore, one may expect a large gradient of strain from the surface towards the center, and huge strain in the center of such fractal blobs. Arguments in favor of this analysis are the results of He and Thorp[22] who calculated the elastic properties of the random network of tetrahedral atoms with different average coordination $\langle r \rangle$. Their results show that the elastic constants depend predominantly on $\langle r \rangle$ and go to zero when $\langle r \rangle = r_p \approx 2.4$ according to the relation $K \propto (\langle r \rangle - r_p)^{1.5}$. Applying the ratio of elastic constants for the central and surface atoms of the overconstrained fractal blobs with assumption of the full coordination of central atoms ($\langle r \rangle = 4$), we found that the mean coordination number of the surface atoms is $\langle r \rangle = 2.48$, which is just in a critical region of the relaxed network. Therefore, the overcoordinations of atoms in amorphous solids are relaxed through the bond percolation of nanometer-sized fractal blobs. Comparing the relations for the elastic constants on $\langle r \rangle$ and l dependence we found that the mean coordination number of atoms in fractal blobs decreases linearly with volume: $\langle r \rangle = \langle r_p \rangle + (4 - r_p)(a/l)^3$. If it is possible to check this relation by numerical or by explicit calculation, then our assumption of the origin of the fractal in the overconstrained rigid bond percolation regions will be strongly confirmed.

Figure 6 shows the ratio of intensities of the boson peak and the amorphous phase in ion-bombarded GaAs as a function of the applied ion dose. The sum of the intensities of the TA, II A, and LO phonon bands was used for the intensity of the amorphous phase. The TO band was not included in the summation due to its overlap with the crystalline TO(Γ) band. The procedure for the Raman spectrum decomposition was published elsewhere.[50] The fact that the boson peak increases faster than the amorphous phase with applied ion dose, or by increasing the C content in a-$Si_{1-x}C_x$:H shown in Fig. 7 is very hard to explain by the model of multiple-order Raman scattering,[51] but confirms the hypothesis of amorphous solids as a two-phase composite. The spectra in Fig. 7 are due to clearness presented without the other fitted vibrational bands. The incorporation of C atoms in the silicon network can be considered as alloying. For concentrations up to 30 at. %, the carbon bonding is mainly substitutional.[52] This causes, due to lower C diameter, a local strain and a deformation of the network. Also, in addition, one may expect a nucleation of rigid regions at locations of carbon bonding. Therefore, the intensity increase of the boson peak with carbon content can be qualitatively interpreted with increasing number of nanometer-strained fractal regions whose origin should be in the homogeneous substitutional bonding of carbon atoms.

Observation of fractal vibrations at frequencies which are well above the acoustical phonon vibrations is not clear enough and needs explanation. According to fractal theory, the fracton range of vibration is expected from the frequency ω_{co1} to the so-called fracton Debye frequency: $\omega_{FD} = \omega_{co1}(\xi/a)^{D/\tilde{d}}$.[20] The apparent Debye frequency as projected by the low-frequency velocity of sound is given by $\omega_D = \omega_{co1}(\xi/a)$. For the shortest length scale in the fractal, we use the distance between identical atoms: in a-Si, $a = 2.35$ Å, while in a-GaAs, $a = 4$ Å. Table II shows the comparison of the calculated values of ω_D and ω_{FD} for a-Si:H and a-GaAs with the crystalline Debye frequency ω_D and estimated value for ω_{FD} based

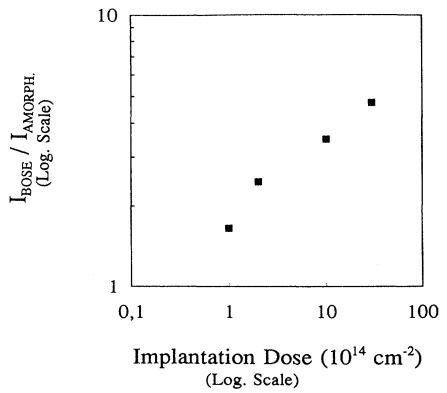

FIG. 6. Ratio of intensities of boson peak and amorphous phase (sum of TA, II A, and LO phonon bands) in dependence on applied Si^+ ion doses.

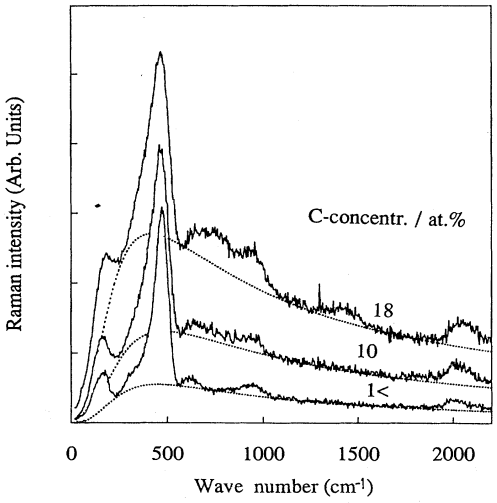

FIG. 7. Boson peak in temperature reduced and radiometrically corrected Raman spectra of *a*-SiC:H.

on observed deviation of experimental data in the Raman spectra from the expected spectral shape of fracton vibrations. In spite of our crude analysis the apparent agreement is good. As a possible origin of apparent deviation at ω_{FD} we have not ruled out photoluminescence, but nevertheless, contrary to other models for the explanation of the boson peak, the high-frequency tail of the boson peak is, according to our knowledge, only well explained by the fractal model.

Experimentally observed anomalies in amorphous silicon such as transient photoconductivity, linear variations in the density of electronic states, and dependence of dc conductivity upon the hydrogen content were qualitatively explained using the fractal geometry.[33] Here, by applying the fractal model we will explain some other experimentally observed anomalies in amorphous semiconductors, too.

A. Sound velocity in tetrahedral amorphous semiconductors

An anomalously low value of the sound velocity v_s was observed in tetrahedral amorphous semiconductors.[44] For example, in sputtered amorphous Ge and Si thin films, while the expected sound velocities should be somewhat less than in the crystalline state, the observed values were only 55–60 % of the *c* state. In the fractal model v_s is scaled with density ρ according to the relation $v_s \propto \rho^{(D/\bar{d}-1)/(\bar{d}-D)}$.[43] With the density of the amorphous state of $\approx 90\%$ of the *c* state, and the mentioned values for fractal and spectral dimensions, we found that the sound velocity in the *a* state is 64% of the *c* state, which is in good agreement with the observed values.

TABLE II. Debye frequency ω_D and fracton Debye frequency ω_{FD} calculated from the fracton model. For a comparison a crystalline Debye frequency and the frequency of observed deviation from the fracton scattering regime are presented.

	ω_D (cm^{-1})	ω_D (cryst.) (cm^{-1})	ω_{FD} (cm^{-1})	ω_{FD} (obser.) (cm^{-1})
Si	625	445	3987	≈ 3400
GaAs	228	250	946	≈ 1000

B. Quenching in As_2S_3

Changes in the phonon density of states $g(\omega)$, in neutron inelastic scattering, and in the coupling constant $C(\omega)$, of Raman-scattering intensity found in As_2S_3 after quenching, shows a negligible variation of structure on a short-range scale, but significant influence on the structural properties at the MRO.[53] The estimated changes in Raman scattering intensity $I(\omega)$ have been related to changes in $g(\omega)$ according to the relation $I_{quen}/I_{ann} \approx (g_{quen}/g_{ann})^{1.8}$. In the fractal model, assuming that changes in phonon density of states are caused mainly by changes in spectral dimension which is a reasonable assumption due to its sensitivity on local microstructure, the ratio of Raman-scattering intensity of quenched and annealed sample should be $I_{quen}/I_{ann} \approx (g_{quen}/g_{ann})^{2(\sigma+d-D)/D}$. Using the mentioned values for parameters of the fractal, we get the value 1.3 for the exponent. But if we use $D=2.2$ instead $D=2.5$, we get the same value as observed. Therefore, the quenching effects on Raman and inelastic neutron scattering can be qualitatively explained by changes in spectral dimension of the fractal blobs embedded in continuous random network structure.

V. MEDIUM-RANGE ORDER IN AMORPHOUS SEMICONDUCTORS

In contrast to tetrahedral semiconductors, the vitreous amorphous semiconductors are glasses in the strictest sense. They can be formed by quenching from the melt, they possess a glass transition temperature at which softening occurs, and there is a continuity of properties from the glassy solid to the true nonviscous liquid. It is believed that the origin of the structural difference between vitreous and tetrahedral amorphous semiconductors is in local arrangements of atoms at a length scale of few interatomic distance. The correlation length of MRO can be evaluated from the crossover frequency of the boson peak using the characteristic length scale $\xi = v_s/(\omega_{co1}c)$, and from the position Q_1 of the first sharp diffraction peak observed in the structure factor $S(Q)$ of inelastic x-ray and neutron scattering using the equivalent distance $R = 2\pi/Q_1$.[3–5,54,55] In Table III we give the values of Q_1 and ω_{co1} for a number of vitreous and tetrahedral amorphous semiconductors together with the calculated values for the correlation length of MRO normalized to the first interatomic distance (ξ^1). Figure 8 shows the comparison of ξ^1 obtained from the FSDP and boson peak. Agreement of ξ^1 obtained from the boson peak with the values deduced from the FSDP in tetrahedral amorphous semiconductors additionally confirms our interpretation of the BBS as boson peak. From Fig. 8 it is evident that the correlation lengths of MRO in tetrahedral amorphous semiconductors are 3–4 times shorter than in vitreous semiconductors. Shorter

TABLE III. Experimental values of position of FSDP, Q_1, boson peak frequency ω_{co1}, first interatomic distance r_1, and velocity of sound v_s in some amorphous semiconductors. Values ξ^1_{FSDP} and ξ^1_{BOSE} represent the scale of medium-range order which we define as correlation length of MRO normalized onto first interatomic distance.

Material	Q_1 (Å^{-1})	ω_{co1} (cm^{-1})	r_1 (Å)	v_s (ms^{-1})	$\xi_{FDSP}=2\pi/(Q_1 r_1)$	$\xi_{BOSE}=v_s/(2\omega_{co1} r_1 c)$
Si	1.95[a]	245[b]	2.35[c]	4400[d]	1.37	1.27
GaAs	1.89[e]	120[b]	2.45[c]	2730[f]	1.36	1.55
Se	1.4[g]	18[g]	2.25[g]	1050[h]	1.99	4.32
As_2Se_3	1.23[g]	24[h]	2.55[g]	1440[h]	2.00	3.92
As_2S_3	1.26[g]	26[h]	2.25[g]	1650[g]	2.22	4.70
GeS_3	1.04[i]	22[h]	2.23[i]	2030[h]	2.71	6.9
$GeSe_3$	1.01[i]	20[h]	2.38[i]	1820[j]	2.61	6.37
$SiSe_3$	1.02[g]	9[g]	2.3[g]	800[g]	2.68	6.44

[a]Reference 54.
[b]Our values.
[c]Reference 56.
[d]Reference 25.
[e]Value for Ge, Ref. 55.
[f]Reference 50.
[g]Reference 55.
[h]Reference 8.
[i]Reference 3.
[j]Reference 57.

correlation length means faster disappearance of structural order, which should result in larger internal strain of ordered nanoregions (blobs). As a consequence a broken bond should appear inside and at boundaries of such blobs increasing the concentration of the dangling bonds which are in a large number observed in tetrahedral amorphous semiconductors. Due to large strain an impurity atom inside the nanometer blobs will not be able to rearrange the local environment and, therefore, will change its coordination. This will provide the conditions for appearance of the impurity level and, therefore, explain the possibility of doping of tetrahedral amorphous semiconductors. In the melt phase, the large strain connected with the structure of the blobs will prevent their formation. This fact is confirmed by inelastic diffraction scattering on Si where in the melt phase only the presence of short range was observed.[54] As a consequence, it will not be possible to create an amorphous phase by quenching from liquid.

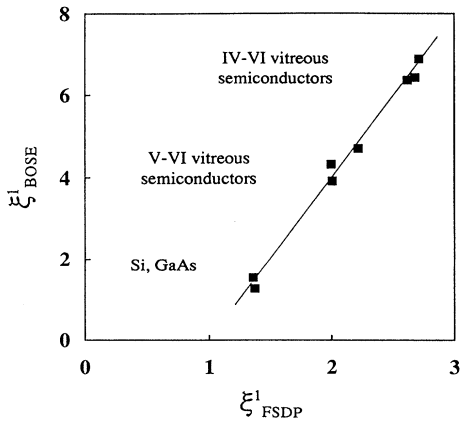

FIG. 8. Correlation of scales of MRO, ξ^1, obtained from boson peak and FSDP. Line is drawn for a visual aid.

Thus, the analysis of correlation length of MRO permits one to conclude that the spatial relaxation of structural order is sharply different for materials which fall into two different classes of amorphous semiconductors. This difference permits one to explain some properties of tetrahedral amorphous semiconductors that differ from those of vitreous semiconductors: larger internal strain, higher concentration of dangling bonds, possibility of doping, and impossibility of quenching from the melt phase.

VI. CONCLUSION

The intention of our paper is to give evidence of the existence of the boson peak in *a*-GaAs with generalization to tetrahedral amorphous semiconductors, and to confirm the applicability of the fractal theory for the explanation of the boson peak as well. The summary of our results are as follows.

(1) The boson peak in *a*-GaAs is observed.

(2) The similarity of the boson peaks that are observed in different tetrahedral amorphous semiconductors and that are prepared by different methods show their common origin.

(3) Besides the amorphous phase which is usually considered as a CRN, a phase which corresponds to the boson peak is found in tetrahedral amorphous semiconductors.

(4) The properties of the boson peak, such as depolarization ratio, spectral shape, high-frequency tail, and some anomalies found in amorphous semiconductors, are explained by the fractal model.

(5) The origins of the fractals in amorphous solids are discussed in terms of strained nanometer blobs of host atoms whose overcoordination is relaxed through bond percolation.

(6) The correlation length of MRO in tetrahedral amorphous semiconductors is found to be 3–4 times shorter than in vitreous semiconductors. This fact is

used for the explanation of a number of differences between their properties.

The discovery of the boson peak in the form of a phase in tetrahedral amorphous semiconductors may throw a new light upon the structure and medium-range order of amorphous semiconductors.

ACKNOWLEDGMENTS

We would like to thank T. E. Haynes and D. Gracin for supplying the samples. One of the authors (M.I.) wishes to thank L. Colombo, K. Furić, and U. V. Desnica for their interest and encouragement. This research was supported by the Alexander von Humbolt Foundation.

*Permanent address: Ruđer Bošković Institute, Bijenička c. 54, 41000 Zagreb, Croatia.

[1]J. C. Phillips, Phys. Today **35**, (2), 27 (1982).
[2]S. R. Elliot, Phys. Rev. Lett. **67**, 711 (1991).
[3]S. R. Elliot, J. Non-Cryst. Solids **150**, 112 (1992).
[4]S. R. Elliot, Europhys. Lett. **19**, 201 (1992).
[5]V. K. Malinovsky, V. N. Novikov, and A. P. Sokolov, J. Phys. Condens. Matter **4**, 139 (1992).
[6]A. Boukenter, B. Champagnon, E. Duval, J. Dumas, J. F Quinson, and J. Seughetti, Phys. Rev. Lett. **57**, 2391 (1986).
[7]R. J. Nemanich, Phys. Rev. B **16**, 1655 (1977).
[8]W. B. Jackson, S. J. Oh, C. C. Tsai, and J. W. Allen, Phys. Rev. Lett. **53**, 1481 (1984).
[9]J. J. Freeman and A. C. Anderson, Phys. Rev. B **34**, 5684 (1986).
[10]J. E. Graebner and B. Golding, Phys. Rev. B **34**, 5788 (1986).
[11]J. E. Graebner, B. Golding, and L. C. Allen, Phys. Rev. B **34**, 5696 (1986).
[12]A. P. Sokolov, A. P. Shebanin, O. A. Golikova, and M. M. Mezdrogina, J. Phys. Condens. Matter **3**, 9887 (1991).
[13]R. Shuker and R. W. Gammon, Phys. Rev. Lett. **25**, 222 (1970).
[14]U. Buchenau, M. Prager, N. Nücker, A. J. Dianoux, N. Ahmad, and W. A. Philips, Phys. Rev. B **34**, 5665 (1986).
[15]V. K. Malinovsky, V. N. Novikov, and A. P. Sokolov, Phys. Lett. A **153**, 63 (1991).
[16]V. K. Malinovsky, V. N. Novikov, P. P. Parshin, A. P. Sokolov, and M. G. Zemljanov, Europhys. Lett. **11**, 43 (1990).
[17]A. P. Sokolov, A. Kisliuk, M. Soltwisch, and D. Quitmann, Phys. Rev. Lett. **69**, 1540 (1992).
[18]A. Boukenter, E. Duval, and H. M. Rosenberg, J. Phys. C **21**, L541 (1988).
[19]J. E. de Oliveira, J. N. Page, and H. M. Rosenberg, Phys. Rev. Lett. **62**, 780 (1989).
[20]S. Alexander, C. Laermans, R. Orbach, and H. M. Rosenberg, Phys. Rev. B **28**, 4615 (1983); A. Aharony, S. Alexander, O. Entin-Wohlman, and R. Orbach, Phys. Rev. Lett. **58**, 132 (1987).
[21]E. Courtens, R. Vacher, and E. Stoll, Physica D **38**, 41 (1988).
[22]*Amorphous Semiconductors,* edited by M. H. Brodsky (Springer, Berlin, 1979); N. F. Mott and E. A. Davis, *Electron Processes in Non-Crystalline Materials* (Clarendon, Oxford, 1979); H. He and M. F. Thorpe, Phys. Rev. Lett. **54**, 2107 (1985).
[23]V. K. Malinovsky, V. N. Novikov, and A. P. Sokolov, J. Non-Cryst. Solids **114**, 61 (1989).
[24]M. H. Brodsky, in *Light Scattering in Solids I,* edited by M. Cardona (Springer-Verlag, Berlin, 1983), p. 205.
[25]M. Ivanda, Phys. Rev. B **46**, 14 893 (1992).
[26]T. E. Haynes and O. W. Holland, Appl. Phys. Lett. **58**, 62 (1991).
[27]N. J. Tao, G. Li, X. Chen, W. M. Du, and H. Z. Cumminis, Phys. Rev. A **44**, 6665 (1991).
[28]C. C. Yu, Phys. Rev. Lett. **63**, 1160 (1989).
[29]V. G. Karpov, M. I. Klinger, and F. N. Ignatiev, Zh. Eksp. Teor. Fiz. **84**, 760 (1983) [Sov. Phys. JETP **57**, 439 (1983)].
[30]R. Orbach, Science **231**, 814 (1986).
[31]Ph. Dumas, B. Bouffakhreddine, C. Arma, O. Vatel, E. Andre, R. Galindo, and F. Salvan, Europhys. Lett. **22**, 717 (1993).
[32]R. C. Salvarezza, L. Vazquez, P. Herrasti, P. Ocon, J. M. Vara, and A. J. Arvia, Europhys. Lett. **20**, 727 (1992).
[33]R. D. McLeod and H. C. Card, J. Non-Cryst. Solids **105**, 17 (1988).
[34]A. Avogadro, S. Aldrovandi, F. Borsa, and G. Carini, Philos. Mag. B **56**, 227 (1987).
[35]S. Alexander, O. Entin-Wohlman, and R. Orbach, Phys. Rev. B **34**, 2726 (1986).
[36]A. Jagannathan, R. Orbach, and O. Entin-Wohlman, Phys. Rev. B **39**, 13 465 (1989).
[37]T. Achibat, A. Boukenter, E. Duval, G. Lorentz, and S. Etienne, J. Chem. Phys. **95**, 2949 (1991).
[38]V. N. Novikov, A. P. Shebanin, V. P. Azarenkov, A. V. Baibak, Yu. V. Krmarenko, and V. P. Privalko, J. Raman. Spectrosc. **25**, 139 (1993).
[39]S. Alexander, Phys. Rev. B **40**, 7953 (1990).
[40]V. Mazzacurati, M. Montagna, O. Pilla, G. Viliani, G. Ruocco, and G. Signorelli, Phys. Rev. B **45**, 2126 (1992).
[41]A. J. Scholten, A. V. Akimov, and J. I. Dijkluis, Phys. Rev. B **47**, 13 910 (1993); A. J. Scholten, A. V. Akimov, P. A. W. E. Verlag, J. I. Dijkluis, and R. S. Meltzer, J. Non-Cryst. Solids **164-166**, 923 (1993).
[42]E. Stoll, M. Kolb, and E. Courtens, Phys. Rev. Lett. **68**, 2472 (1992).
[43]S. Alexander, E. Courtens, and R. Vacher, Physica A **195**, 286 (1993).
[44]L. R. Testardi and J. J. Hauser, Solid State Commun. **21**, 1039 (1977).
[45]R. P. Sharma, R. Bhadra, L. E. Rehn, P. M. Baldo, and M. Grimsdich, J. Appl. Phys. **66**, 152 (1989).
[46]M. Holtz, R. Zallen, O. Brafman, and S. Matteson, Phys. Rev. B **37**, 4609 (1988).
[47]S. Alexander and R. Orbach, J. Phys. (Paris) **43**, L625 (1982).
[48]I. Webman and G. S. Grest, Phys. Rev. B **31**, 1689 (1985).
[49]J. J. Baum, K. K. Gleason, A. Pines, A. N. Garraway, and J. A. Reimer, Phys. Rev. Lett. **56**, 1377 (1986).
[50]M. Ivanda, U. V. Desnica, and T. E. Haynes, Mater. Sci. Forum **143-147**, 1387 (1994).
[51]A. Zwick and R. Carles, Phys. Rev. B **48**, 6024 (1993); A. Chehaidar, A. Zwick, R. Carles, and J. Bandet, *ibid.* **50**, 5345 (1994).
[52]W. Y. Lee, J. Appl. Phys. **51**, 3365 (1980).
[53]S. L. Isakov, S. N. Ishmaev, V. K. Malinovsky, V. N. Novikov, P. P. Parshin, S. N. Popov, A. P. Sokolov, and M. G. Zemlyanov, Solid State Commun. **86**, 123 (1993).
[54]E. A. Chechetkina, J. Phys. Condens. Matter **5**, L527 (1993).
[55]V. N. Novikov and A. P. Sokolov, Solid State Commun. **77**, 243 (1991).
[56]C. Kittel, *Introduction to Solid State Physics* (Wiley, New York, 1971).
[57]S. C. Mass and D. L. Price, in *Physics of Disordered Materials,* edited by D. Adler, H. Fritzsche, and S. R. Ovshinsky (Plenum, New York, 1985).